

# An EEG-based approach for Parkinson's disease diagnosis using Capsule network

Shujie Wang<sup>1</sup>, Gongshu Wang<sup>1</sup>, Guangying Pei<sup>1</sup>

<sup>1</sup> School of Life Science, Beijing Institute of Technology, Haidian District, Beijing, China

**Abstract:** As the second most common neurodegenerative disease, Parkinson's disease has caused serious problems worldwide. However, the cause and mechanism of PD are not clear, and no systematic early diagnosis and treatment of PD have been established, many patients with PD have not been diagnosed or misdiagnosed. In this paper, we proposed an EEG-based approach to diagnosing Parkinson's disease, it mapping the frequency band energy of EEG signals to 2-dimensional images using the interpolation method and identifying classification using CapsNet, achieved 89.34% classification accuracy for short-time EEG sections, which exceeds the conventional SVM model. A comparison of separate classification accuracy across different EEG bands revealed the highest accuracy in the gamma bands, suggesting that we need pay more attention to the changes in gamma band changes in the early stages of Parkinson.

**Keywords:** Parkinson's disease; machine learning; deep learning; electroencephalograph; capsule network

## I Introduction

Parkinson's disease (PD) is the second most common neurodegenerative disease worldwide, frequently in the elderly and affecting in 2% – 3% of people over 60[1,2]. According to the global burden of disease study, neurological diseases are currently the major source of disability worldwide, and PD is the fastest growing disease of these diseases (with age-standardized prevalence, disability and mortality). From 1990 to 2015, the number of people with Parkinson's disease worldwide increased by 118% to 6.2 million [3,4]

The main clinical manifestations of PD include delay, limb stiffness, static tremor and gait disorder, in many patients sleep disorders and anxiety. So far, there is no effective treatment means, mainly relying on drug intervention and comprehensive treatment to delay the progress of the disease, but the efficacy of drugs in middle and late gradually decline, and complications gradually appear. Although surgical treatment can be used as a means of middle and late PD treatment, limited clinical application is applied due to invasive treatment and high cost [5]. Therefore, the early diagnosis of PD is particularly important.

However, the cause and mechanism of PD are not clear, and no systematic early diagnosis and treatment of PD have been established. Many patients with PD are not diagnosed or misdiagnosed, resulting in a large number of actual PD patients being unable to receive the corresponding treatment for [6]. The difficulty in early diagnosis of PD is the inconspicuous characteristics and susceptibility to confuse with other diseases[7]. Therefore, how to effectively extract the features in the input signal, and then improve the Parkinson's disease diagnosis accuracy is an important difficulty in PD diagnosis.

Electroencephalography (EEG) can record the spontaneous, rhythmic electrical activity of brain cells, with good temporal resolution and relatively easy to collect, and is widely used in the detection of neurological diseases. Studies show that the most important EEG change in PD patients is the main wave frequency (dominant frequency, DF) from rhythm to slower high rhythm, namely EEG slows down [8]. EEG can be used for the detection of non-motor symptoms, such as EEG studies in PD patients with depressive symptoms showed that increased wave and wave activity [9]. PD motor symptoms are closely

related to the frequency band, continuous motor task completion is related to a specific EEG frequency band, including frequency bands corresponding to movement preparation, movement control and execution corresponding frequency band and conflict signal processing [10-13]. As the main rhythm in the cortical-spinal system, frequency bands are important in coordinating motor function, and motor abnormalities in PD may cause [14,15] by increased high frequency coherence in the mesomotor cortical-subcortical region. Combined, past studies have found that EEG can more objectively and quantitatively represent the disease process and symptoms of PD patients, which can effectively guide the early diagnosis of PD[16-18]. Among these models, convolutional neural networks (CNN) showed superiority in physiological signal recognition[19]. However, the pooling layer in CNN ignores a lot of information because of its data compression functions and static routing, and capsule network(CapsNet) could solve this problem[20]. CapsNet considers the spatial relationships between features, simulated the human brain learning process, and achieved the best results in the MNIST dataset.

In this paper, we propose an EEG-based approach for Parkinson’s disease diagnosis with capsule network. First, we project the energy features of the different frequency bands of the EEG to the corresponding spatial positions by the interpolation method to construct the EEG map of the different frequency bands, that the raw signals of EEG are converted to 2D image; and then enter the EEG maps into CapsNet for training and testing. To our best current knowledge, it is the first attempt to diagnose Parkinson’s disease with capsule network.

## II Materials and Methods

### A Subjects

85 participants were recruited from November 2019 to January 2021 in the present study. 55 nondemented Parkinson's disease patients were recruited from the Neurological Rehabilitation Center of Beijing Rehabilitation Hospital Affiliated to Capital Medical University and 30 healthy controls were recruited by the local community is recruiting ads. Demographic and clinical details are summarized in Table.1. This study was approved by the Ethics Committee of the Beijing Rehabilitation Hospital Affiliated to Capital Medical University and Aero-space Central Hospital following the Declaration of Helsinki, and all participants were given informed written consent before the experiment.

Table. 1 Demographic data.

|                   | PD            | HC           | P-value |
|-------------------|---------------|--------------|---------|
| N (sex ratio M/F) | 55 (29/26)    | 30 (15/15)   | 0.813   |
| Age (SD), y       | 59.82 (7.33)  | 57.73 (7.63) | 0.226   |
| MMSE (SD)         | 27.35 (1.71)  | 27.53 (2.50) | 0.888   |
| Education         | 4.24 (0.94)   | 3.9 (1.22)   | 0.198   |
| UPDRS III(SD)     | 30.42 (12.52) | -            | -       |
| MoCA (SD)         | 25.52 (3.27)  | -            | -       |
| H&Y (SD)          | 2.25 (0.49)   | -            | -       |

MMSE, Mini-Mental State Examination; UPDRS III, Movement Disorders Society-Unified Parkinson’s Dis-ease Rating Scale-Part III (severity of motor symptoms); MoCA, Beijing version of the Montreal Cognitive Assessment; H&Y, Hoehn & Yahr stage;

### B Data

Using the BP Company 32 Guide EEG Acquisition Equipment (Brain products, Germany) for EEG data acquisition, The EEG acquisition is based on the International 10/20 system, EEG was collected from 30 channels (FP1, FP2, F7, F3, Fz, F4, F8, T3, C3, Cz, C4, T4, T5, P3, Pz, P4, T, T6, FT9, FC5, FC1, CP5, CP1, Oz, CP6, CP2, FT10, FC6, FC2, O1 and O2);The reference electrode was set as the left

and right papillary electrodes (TP9, TP10); The Grounding electrode is placed in front of it; The sampling rate was 1,000 Hz; The scalp impedance was all reduced to 5 kΩ at the acquisition. Eye-open and closed resting EEG signals were collected simultaneously for each subject for 15min each.

The EEG signal preprocessing mainly includes the following steps: data preview, electrode positioning, filtering, Independent Component Analysis (ICA), artifact deletion, and segmentation. The first step ,electrode re-reference, using double electrode reference to reduce the error and brain hemisphere effect caused by the single reference electrode; the data are filtered from high-frequency band and working frequency interference baseline drift by 0.5 Hz high-pass and 45 Hz low-frequency FIR filter; then use ICA to remove noise components such as EMG and EMO to obtain relatively pure EEG signals;

Considering the inherent structure of the data in space, frequency, and time, we used a method proposed in Pouya Bashivan et al. in order to transform the measurements into a 2-D image to save the spatial structure and used multiple color channels to represent the spectral dimension[21]. the energy features of frequency band in each channel were calculated by Welch method, and the electrode 3 D coordinates were extracted from the equipment information; Azimuthal Equidistant Projection(AEP) to project the electrode position to 2 D plane; finally, the scattering power measurement on the scalp was interpolated for EEG feature image of 8 (four band energy characteristics and two eye-open states)×32 ×32 (32×32 grid) .Thus, the topographic features of the EEG spectrum energy are retained, which is more conducive as the input of the subsequent deep learning model.

### C CapsNet

Capsule network is a neural network instead of scalar neurons of convolutional neural network (CNN), which can better capture and characterize the relationship between the characteristic attributes of the input signal (such as relative location, scale, direction, etc.).The CapsNet model retains the convolutional properties of the convolutional neural network, creates higher-level capsules to cover a larger region of the image, and does not lose the exact location information within the region, while combining the capsules with dynamic routing, improving the efficiency of the capsule network.

Unlike the scalar neurons in the convolutional neural network, the capsule  $j$  (vector neuron  $j$ ) in the capsule network uses a matrix  $W_{ij}$  to process the input vector  $u_i$  into new input vectors  $\hat{u}_{j|i}$

$$\hat{u}_{j|i} = W_{ij} u_i \quad (1)$$

The input vector  $\hat{u}_{j|i}$  is then multiplied by the weight  $c_{ij}$ , and the total input of the capsule  $j$  is obtained after the sum of the weighted vector

$$s_j = \sum_i c_{ij} \hat{u}_{j|i} \quad (2)$$

Using a nonlinear "squashing" function as activation to ensure that the capsule output vector  $v_j$  is between 0-1, so that  $v_j$  could represent the probability that the entity represented by the capsule is present in the current input.

$$v_j = \frac{\|s_j\|^2}{1 + \|b_j\|^2} \frac{s_j}{\|s_j\|} \quad (3)$$

The weight  $c_{ij}$  in (2) is the coupling coefficients determined by the iterative dynamic routing process. The sum of the coupling coefficient between all the  $k$  capsules of the capsule  $i$  and the upper layer is 1.  $c_{ij}$  is decided by the ‘‘Routing softmax’’

$$c_{ij} = \frac{\exp(b_{ij})}{\sum_k \exp(b_{ik})} \quad (4)$$

In (3),  $b_{ij}$  is the log-prior probability that the capsule  $i$  should be coupled to the capsule  $j$ .  $b_{ij}$  obtained by distinction learning as with all other weights, it depends on the location and type of the two capsules rather than the current input. For the first capsule layer, the initial value of  $b_{ij}$  is 0, for capsule  $I$  in layer  $l$  and capsule  $j$  in layer  $(l+1)$

$$b_{ij} \leftarrow b_{ij} + \hat{u}_{j|i} \cdot v_j \quad (5)$$

#### D Proposed method

As shown in Fig. 1. The specific implementation scheme is to obtain the EEG feature image of  $N$  (it turns on the frequency band energy features and eye-open states)  $\times 32 \times 32$  ( $32 * 32$  grid) as input, and then passes through the standard convolutional layer, main capsule layer and digital capsule layer.

The first layer is the ordinary CNN layer, which acts as a pixel-level local feature detection. The input is  $N \times 32 \times 32$  in size, and the first layer uses 256 convolutional  $9 \times 9$  cores with a stride of 1 and ReLU activation, resulting in an output matrix size of  $24 \times 24 \times 256$ .

The second layer is the main capsule layer (Primarycaps), which can be understood as a stack of 8 parallel conventional convolutional layers with  $8 \times 32$  convolution  $9 \times 9$  cores with step size of 2, yielding 8 output matrices of  $8 \times 8 \times 1 \times 32$ , changing the 3 D output tensor  $6 \times 6 \times 1 \times 32$  under the traditional convolution to the 4 D output tensor  $6 \times 6 \times 8 \times 32$ , that is, each calculated output is a vector of length 8.

The third digital capsule layer (Digitcaps) spreads and routing updates based on the vector output of the second layer. The second layer outputs a total of  $8 \times 8 \times 32 = 2048$  vectors, each with a dimension of 8, namely, 2048 Capsule units in layer  $i$ . While the third layer  $j$  has 2 standard Capsule units, the output vector for each Capsule has 16 elements. The number of Capsule cells in the previous layer is 2048, so there will be  $2048 \times 2$ , and each with a dimension of  $8 \times 16$ . When the predicted vectors are multiplied with the counterpart, we have  $2048 \times 2$  coupling coefficients, and the corresponding weighted sum yields 2161 input vectors. The input vector is input into the ‘‘squashing nonlinear function to obtain the final output vector, where the length indicates the probability of identification as a category.

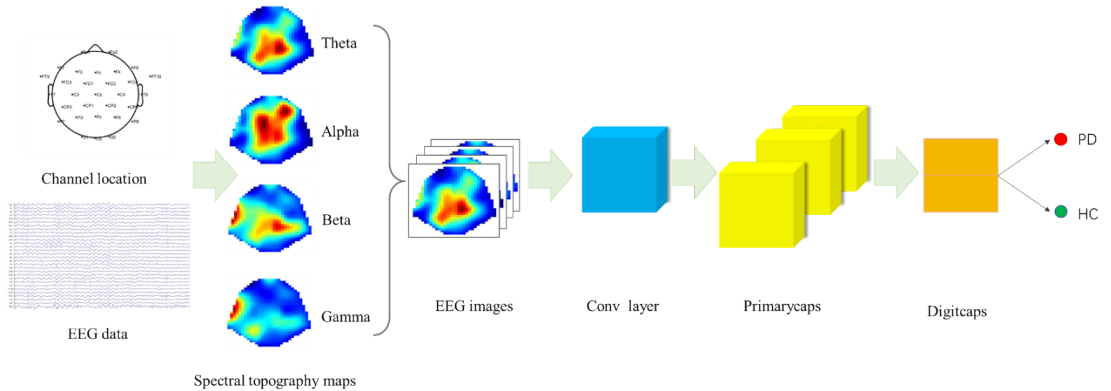


Fig. 1. Overview of our approach

### III Resultss

In our study, we compare the CapsNet classification results with combined input between different and four bands, evaluate the contribution of different bands to the model, and show that the performance of the model learning increases and the performance of the classification model increases with increasing frequency bands. As shown in table 2, with single band feature , we obtained a 5-fold cross-validated accuracy of 83.85% for gamma band, 82.48% for beta band, 82.58% for alpha band and 82.49% for theta band. It suggest that we need to value the role of the gamma frequency band in Parkinson's pathology .

Table.2 The performance of classification for different band inputs

| feature | Accuracy    | Sensitivity | Specificity |
|---------|-------------|-------------|-------------|
| theta   | 82.49±3.07% | 78.71±6.07% | 86.28±6.22% |
| alpha   | 82.58±3.76% | 78.40±4.40% | 86.75±5.75% |
| beta    | 82.48±3.69% | 75.84±3.21% | 89.13±7.83% |
| gamma   | 83.85±4.76% | 82.16±5.23% | 85.54±8.05% |
| all     | 89.34±4.06% | 86.88±4.10% | 91.83±6.76% |

As shown in table 3, we got a significant increase in accuracy, 89.34% for all bands feature input (Four frequency band energy features and two eye-open states). It has exceeded the classification accuracy of 88.99% with multi-kernel SVM algorithm proposed by our team before[18].

Table.3 The performance of classification for different approach

| feature | Accuracy    | Sensitivity | Specificity |
|---------|-------------|-------------|-------------|
| SVM     | 88.99±4.11% | 86.45±7.14% | 91.54±3.89% |
| CapsNet | 89.34±4.06% | 86.87±4.10% | 91.83±6.76% |

### IV Conclusion

In this paper, we proposed a method to diagnose parkinson's disease by EEG-based CapsNet. As a neural network model, this method has exceeded the classification accuracy of svm model in small samples (trained less than 100), and has the potential to identify Parkinson's disease electrophysiological signal characteristics and build a dynamic mapping model of Parkinson's disease patients, which can serve as an effective supplement to the current clinical Parkinson's diagnosis. Moreover, the good performance of gamma band suggest that we need to value the role of the gamma frequency band in Parkinson's pathology.

### References

- [1] Lees A J, Hardy J, Revesz T. Parkinson's disease [J]. Lancet, 2009, 373(9680): 2055-66.
- [2] Poewe W, Seppi K, Tanner C M, et al. Parkinson disease [J]. Nat Rev Dis Primers, 2017, 3(21)..
- [3] Global, regional, and national burden of neurological disorders during 1990-2015: a systematic analysis for the Global Burden of Disease Study 2015. GBD 2015
- [4] Neurological Disorders Collaborator Group. Lancet Neurol. 2017 Nov; 16(11):877-897.
- [5] Ferrazzoli D, Carter A, Ustun FS, et al. Dopamine replacement therapy, learning and reward

prediction in Parkinson's disease: implications for rehabilitation [J]. *Front Behav Neurosci*, 2016, 10(6): 121.

[6] Weingarten, C. P., Sundman, M. H., Hickey, P., & Chen, N. K. (2015). Neuroimaging of Parkinson's disease: Expanding views. *Neuroscience & Biobehavioral Reviews*, 59, 16-52.

[7] Tolosa, E., Wenning, G., Poewe, W., 2006. The diagnosis of Parkinson's disease. *Lancet Neurol.* 5, 75–86.

[8] Geraedts V J, Boon L I, Marinus J, et al. Clinical correlates of quantitative EEG in Parkinson disease A systematic review [J]. *Neurology*, 2018, 91(19): 871-83.

[9] 冀伟. 伴与不伴抑郁帕金森病患者脑电功率对比研究. *中国实用神经疾病杂志*[J]. 2014, 17(13): 47-9.

[10] Haynes W I A, Haber S N. The Organization of Prefrontal-Subthalamic Inputs in Primates Provides an Anatomical Substrate for Both Functional Specificity and Integration: Implications for Basal Ganglia Models and Deep Brain Stimulation [J]. *J Neurosci*, 2013, 33(11): 4804-14.

[11] Cavanagh J F, Figueroa C M, Cohen M X, et al. Frontal Theta Reflects Uncertainty and Unexpectedness during Exploration and Exploitation [J]. *Cereb Cortex*, 2012, 22(11): 2575-86.

[12] Georgiev D, Lange F, Seer C, et al. Movement-related potentials in Parkinson's disease [J]. *Clinical Neurophysiology*, 2016, 127(6): 2509-19.

[13] Bockova M, Rektor I. Impairment of brain functions in Parkinson's disease reflected by alterations in neural connectivity in EEG studies: A viewpoint [J]. *Clinical Neurophysiology*, 2019, 130(2): 239-47.

[14] Muslimovic D, Post B, Speelman J D, et al. Determinants of disability and quality of life in mild to moderate Parkinson disease [J]. 2008, 70(23): 2241-7.

[15] Mak M K, Wong-Yu I S, Shen X, et al. Long-term effects of exercise and physical therapy in people with Parkinson disease [J]. *Nat Rev Neurol*, 2017, 13(11): 689-703.

[16] BI, Xiaojun; WANG, Haibo. Early Alzheimer's disease diagnosis based on EEG spectral images using deep learning. *Neural Networks*, 2019, 114: 119-135.

[17] GEMEIN, Lukas AW, et al. Machine-learning-based diagnostics of EEG pathology. *NeuroImage*, 2020, 220: 117021.

[18] GUO, Guoxin. Diagnosing Parkinson's Disease Using Multimodal Physiological Signals. In: *Human Brain and Artificial Intelligence: Second International Workshop, HBAI 2020: Held in Conjunction with IJCAI-PRICAI 2020, Yokohama, Japan, January 7, 2021: Revised Selected Papers*. Springer Nature, 2021. p. 125.

[19] Rim B, Sung N J, Min S, et al. Deep Learning in Physiological Signal Data: A Survey [J]. *Sensors (Basel, Switzerland)*, 2020, 20(4).

[20] SABOUR, Sara; FROSST, Nicholas; HINTON, Geoffrey E. Dynamic routing between capsules. *arXiv preprint arXiv:1710.09829*, 2017.

[21] BASHIVAN, Pouya, et al. Learning representations from EEG with deep recurrent-convolutional neural networks. *arXiv preprint arXiv:1511.06448*, 2015.